Application of Nanotechnology for Heavy Oil Upgrading: Catalytic Steam Gasification/Cracking of Asphaltenes

ARTICLE *in* ENERGY & FUELS · MARCH 2011

Impact Factor: 2.79 · DOI: 10.1021/ef2001772

3 AUTHORS, INCLUDING:

Nashaat N Nassar
The University of Calgary
64 PUBLICATIONS **885** CITATIONS
SEE PROFILE

Azfar Hassan
The University of Calgary
36 PUBLICATIONS **386** CITATIONS
SEE PROFILE

energy&fuels

ARTICLE

pubs.acs.org/EF

Application of Nanotechnology for Heavy Oil Upgrading: Catalytic Steam Gasification/Cracking of Asphaltenes

Nashaat N. Nassar,*[,†,‡] Azfar Hassan,[†,‡] and Pedro Pereira-Almao*[,†,‡]

[†]Alberta Ingenuity Centre for In-Situ Energy, and [‡]Department of Chemical and Petroleum Engineering, University of Calgary, Calgary, Alberta T2N 1N4, Canada

ABSTRACT: Nanotechnology is a rapidly growing technology with considerable potential applications and benefits. Among the numerous applications of nanotechnology for energy and the environment, adsorption, oxidation, and gasification/cracking of asphaltenes, a problematic constituent present in heavy oil, on nanoparticle surfaces are one of the most recent examples. In this work, three different types of metal oxide nanoparticles, namely, Fe_2O_3, Co_3O_4, and NiO, were selected for asphaltene adsorption and catalytic steam gasification/cracking. Adsorption and gasification of asphaltenes were studied using thermogravimetric analysis. The nanoparticles were found to be very efficient for asphaltene adsorption and catalytic steam gasification/cracking. Asphaltene adsorption affinity on the surface of nanoparticles followed the following order: NiO > Co_3O_4 > Fe_2O_3. The catalytic steam gasification/cracking of asphaltenes in the presence of nanoparticles followed the same order as well. The calculated percent conversion at the onset temperature for NiO, Co_3O_4, and Fe_3O_4 nanoparticles was 37, 32, and 21%, respectively. A relationship between adsorption affinity and catalytic activity is also found to exist.

1. INTRODUCTION

It is well-known that oilsands processing and production faces several challenges that need to be surmounted to make it an environmentally sound and economically feasible industry.[1] These challenges include (a) the reduction in capital and operating costs, (b) the improvement of synthetic crude quality to meet stringent market specifications, (c) the reduction of natural gas consumption for H_2 production, (d) the reduction in the amount of diluent volume required to achieve bitumen specifications for transportation, and (e) the reduction of greenhouse gas emissions, especially CO_2 emissions. Nonetheless, a number of possible solutions have been addressed, especially for minimizing the hydrogen production from natural gas and diluent consumption, namely, (i) the use of viscosity reducers, (ii) the development of new sources of hydrogen, such as coal/coke gasification, (iii) heated pipelines, (iv) partial or total upgrading in the field, and (v) diluent return loops.[2−4] Nevertheless, all of these possible solutions have been found to be limiting, because of the high capital and operating costs and/or the ineffectiveness in meeting the environmental regulations.

In this work, we are exploring a novel method for the elimination of asphaltenes, waste hydrocarbons, by adsorption on nanoparticles and, subsequent, catalytic steam gasification of the adsorbed asphaltenes for synthesis gas production. Recently, we investigated the adsorptive removal of asphaltenes from heavy oil solutions by different types of metal oxide nanoparticles.[5,6] Our results showed that a significant amount of asphaltenes was adsorbed onto nanoparticles in a very short time. This current investigation explores the effectiveness of different nanoparticles in catalytic steam gasification of adsorbed asphaltenes. To the best of our knowledge, there has been no research conducted on the catalytic steam gasification/cracking of asphaltenes onto nanoparticles. The present work holds great promise for oilsands recovery and upgrading because the removal of asphaltenes by adsorption and its subsequent catalytic steam gasification would allow for oil upgrading and production of H_2 from waste hydrocarbons. Therefore, this process is a cost-effective and environmentally friendly technique that significantly decreases the waste hydrocarbons, reduces the emission of greenhouse gases, and produces valuable end products.

2. EXPERIMENTAL SECTION

2.1. Nanoparticles. Nanoparticles of Fe_3O_4, Co_3O_4, and NiO were used in this study. Fe_3O_4 was obtained from Nanostructured and Amorphous Materials, Inc., Houston, TX. The other nanoparticles were obtained from Sigma Aldrich Canada, Ltd., Oakville, Ontario, Canada. The textural properties of the nanoparticles, including particle size and Brunauer−Emmett−Teller (BET) and external surface areas, are presented in Table 1.

2.2. Surface Area and Particle Size Measurements. Specific (BET) and external surface areas of nanoparticles were measured by performing nitrogen adsorption and desorption at 77 K, using a Micromeretics Tristar 2000 surface area analyzer. The samples were degassed at 150 °C under N_2 flow overnight before analysis. Surface areas were calculated using the BET equation. External surface areas were obtained by the *t*-plot method. No significant difference between the BET and external surface areas were obtained, indicating that the nanoparticles are essentially nonporous. The size of the nanoparticles was determined using an X-ray Ultima III Multi Purpose Diffraction System (Rigaku Corp., The Woodlands, TX), with Cu Kα radiation operating at 40 kV and 44 mA with a $\theta/2\theta$ goniometer.

2.3. Asphaltenes. Asphaltenes were extracted from Athabasca bitumen with the addition of *n*-heptane at a ratio of 1:40 (g/mL).[5] Precipitated asphaltenes were separated from solution by filtration using

Received: February 1, 2011
Revised: March 21, 2011
Published: March 21, 2011

Table 1. Particle Size and Surface Areas of Selected Metal Oxide Nanoparticles

nanoparticles	X-ray-measured particle size (nm)	specific surface area (BET) (m^2/g)	external surface area (t plot) (m^2/g)
Co_3O_4	22 ± 0.8	41	39
Fe_3O_4	22 ± 1.5	43	37
NiO	12 ± 2.3	107	94

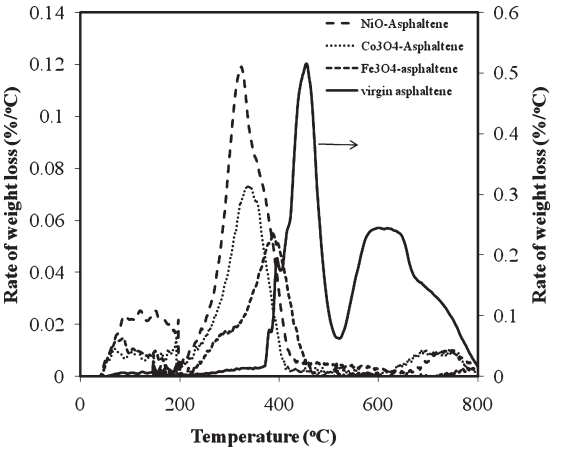

Figure 1. Thermogravimetric/differential thermal analysis (TG/DTA) curves for asphaltene gasification with and without metal oxide nanoparticles. Heating rate, 10 °C/min; air flow, 100 cm^3/min.

an 8 μm Whatman filter paper. The resultant asphaltenes washed thoroughly with *n*-heptane, homogenized, and fined using a pestle and mortar. After that, the asphaltenes were left to dry at room temperature in a hood until no change in mass was observed. The heavy oil model solutions were prepared by redissolving the prepared asphaltenes in toluene at a specified concentration.

2.4. Adsorption of Asphaltenes onto Nanoparticles. Asphaltene adsorption was performed at 25 °C by exposing the heavy oil model solutions to a specified amount of nanoparticles, as explained in our previous study.[5] Nanoparticles containing adsorbed asphaltenes were separated by centrifugation at 5000 rpm for 30 min. After that, the nanoparticles containing adsorbed asphaltenes were dried in a vacuum oven at 60 °C for 24 h. At this stage, the nanoparticles containing adsorbed asphaltenes were ready for the thermal analysis experiment.

2.5. Catalytic Steam Gasification/Cracking of Adsorbed Asphaltenes. Catalytic steam gasification of adsorbed asphaltenes over nanoparticles was carried out and studied using a simultaneous thermogravimetric analysis/differential scanning calorimetry (TGA/DSC) analyzer (SDT Q600, TA Instruments, Inc., New Castle, DE). The instrument has a horizontal beam design that allows flow of gas parallel to the beam as well as above the sample. The system is also equipped with an outlet close to the sample for steam injection. About 10 mg of sample was taken for this analysis. The sample mass was kept low to avoid diffusion limitations. Gasification was performed by first purging the system with Ar at a flow rate of 500 cm^3/min for 10 min, then decreasing the flow rate to 100 cm^3/min, and maintaining this flow throughout the experiment. After the system was purged with Ar for another 20 min at room temperature, the temperature was abruptly raised to 150 °C. At the same time, $H_2O(g)$ was introduced to the system at a flow rate of 6.30 cm^3/min. This flow rate allows the steam to be present above the sample in excess. A plastic syringe containing

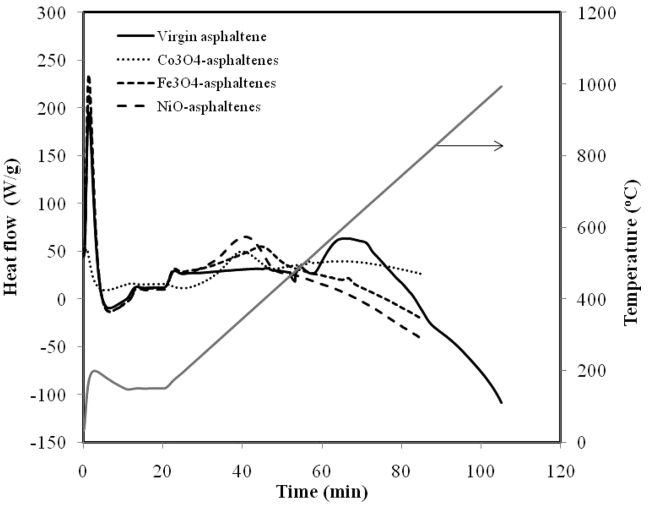

Figure 2. Change in the heat of reaction curves for asphaltene gasification with and without metal oxide nanoparticles. Heating rate, 10 °C/min; air flow, 100 cm^3/min.

distilled water mounted on a syringe pump was used for this purpose. The system was maintained at 150 °C for 20 min to ensure the presence of steam in the vicinity of the asphaltenes adsorbed over nanocatalysts. The system was then heated up to 800 °C at a heating rate of 10 °C/min. The mass and heat changes were recorded. Evolved gases were also analyzed by the Pfeiffer mass spectrometer coupled to the system.

3. RESULTS AND DISCUSSION

3.1. Catalytic Steam Gasification/Cracking of Adsorbed Asphaltenes. Catalytic steam gasification/cracking was performed to obtain more insight about the catalytic effect of nanoparticles using a thermogravimetric setup, as described in the Experimental Section. When simultaneous thermal analysis is performed, both mass and heat changes with time can be monitored. Figure 1 shows the profiles for the rate of mass loss with the increase in the temperature for virgin asphaltenes as well as for asphaltenes adsorbed over nanoparticles. For virgin asphaltene steam gasification/cracking, the mass loss profiles can be divided into three regions: (1) a low-temperature range up to 360 °C, (2) a mid-temperature range from 360 to 500 °C, and (3) a high-temperature range beyond 500 °C. Because asphaltenes are heavy fractions of oil, little mass change is observed during pyrolysis/gasification in the low-temperature range. Because there is very little exothermicity associated with mass loss up to 500 °C in the heat-flow profile (Figure 2), this suggests that complete oxidation of asphaltenes is not the dominant reaction under these conditions. Below 500 °C, the dominant reaction leading to significant mass loss is pyrolysis. However, partial oxidation at low temperatures cannot be ignored.[7] It may be noted in Figure 2 that a spike appears at low time, which is due to the temperature jump from ambient to 150 °C. The decay in the heat-flow profile at long times simply shows that the reaction is already over in the presence of nanoparticles, because no mass loss is seen in Figure 1. However, in the case of virgin asphaltenes, pyrolysis is still occurring at long times (high-temperature region beyond 600 °C) because there is no exothermicity associated with the mass loss in this region. Steam gasification/cracking of virgin asphaltenes without nanoparticles in the presence of steam occurs after 500 °C, as evidenced by the presence of an exotherm

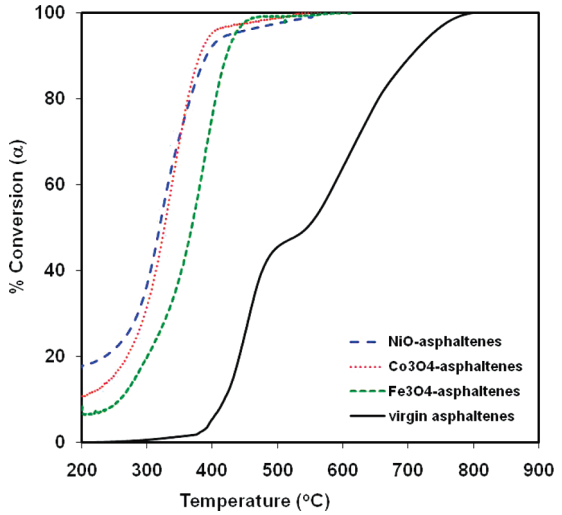

Figure 3. Percent conversion of asphaltenes in the presence and absence of different metal oxide nanoparticles.

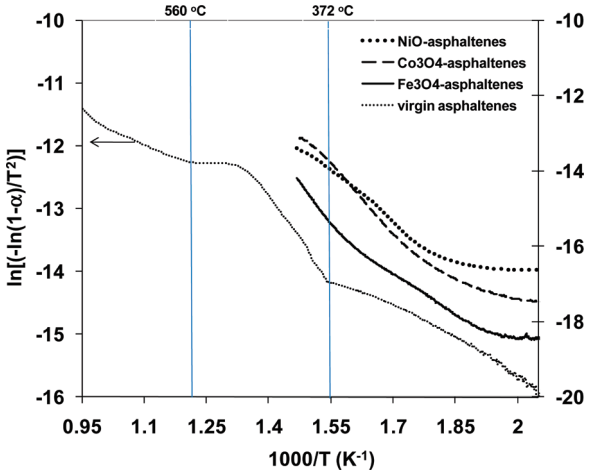

Figure 4. Catalytic steam gasification/cracking of asphaltenes in the presence and absence of different metal oxide nanoparticles.

that follows the mass loss profile shown in Figure 1. The mass loss profile of asphaltenes after adsorption over nanoparticles (Figure 1) shows that steam gasification and/or cracking of asphaltenes occurs at a much lower temperature. From the peak maxima of the mass loss during steam gasification/cracking reactions, it appears that the presence of NiO, Co_3O_4, and Fe_3O_4 nanoparticles lowered the reaction temperature from ~500 to 317, 330, and 380 °C, respectively. This decrease in the reaction temperature validates the idea that these nanoparticles catalyze the gasification/thermal cracking of asphaltenes considerably, with NiO being more active than Co_3O_4 and Fe_3O_4. It may be noted that the mass spectrometry analysis of gases coming out apparently did not show any formation of H_2 or CH_4. This may be due to the low asphaltene content present in the sample taken (less than 10 mg), which was taken to avoid any limitation to diffusion of steam into the sample matrix. Also, we were limited by the sample crucible size (50−60 μL) that allows for holding a small quantity of sample. As a result, the concentration of off-gases remained very dilute and too low to be detected. For this reason, we are labeling this reaction as a catalytic steam gasification/cracking reaction rather than simply calling it a catalytic gasification reaction. Nevertheless, this work proves the catalytic effect of nanoparticles toward such reactions. We believe that gasification is occurring, and our ongoing and future studies involve carrying out gasification studies in a fixed-bed reactor. The results of the fixed-bed study are beyond the scope of this paper.

Figure 3 shows a plot of the percent conversion ratio or the extent of reaction (α) of asphaltenes with and without nanoparticles as a function of the temperature, where α was estimated as per eq 1

$$\alpha = \frac{w_o - w_t}{w_o - w_\infty} \quad (1)$$

where w_o is the initial sample mass, w_∞ is the final sample mass, and w_t is the sample mass at any time. It appears that, in the absence of nanoparticles, steam gasification/cracking commenced beyond 350 °C and appears to occur in two phases: one below and one beyond 500 °C. It is evident from the figure that the presence of nanoparticles greatly enhances the gasification/cracking process, because the reaction onset temperature decreases to temperatures lower than 300 °C. This decrease in the temperature shows the catalytic behavior of nanoparticles for gasification/cracking of asphaltenes. It was interesting to note that, although NiO has the highest surface area, while surface areas of Co_3O_4 and Fe_3O_4 are comparable, the catalytic activity of Co_3O_4 in terms of conversion resembled that of NiO. A similar catalytic activity of nanoparticles with different surface areas shows that the surface area is not the only controlling factor for catalytic activity. This demonstrates that adsorbate−adsorbent interactions are also important and play a role in catalysis, as will be discussed in the following section. It is worth noting that the activity for NiO and Co_3O_4 appears to become almost the same at high temperatures, which may be due to the low asphaltene mass remaining over nanoparticles.

3.2. Estimation of Activation Energies. Activation energies required for the steam gasification reactions of asphaltenes in the presence and absence of nanoparticles can be calculated by processing simultaneous thermal analysis data. For its simplicity, the Coats−Redfern method[8] was employed for estimating the activation energies in this study. The Coats−Redfern method is an integral method of processing the TGA data, which deals with only one weight loss curve to obtain activation energy. The process is as follows.

According to the Arrhenius equation, the conversion rate can be expressed by

$$\frac{d\alpha}{dt} = Ae^{-E_a/RT} f(\alpha) \quad (2)$$

where A is the pre-exponential factor (s^{-1}), E_a is the activation energy (KJ/mol), R is the ideal gas constant (8.314 J mol^{-1} K^{-1}), T is the reaction temperature in Kelvin, and $f(\alpha)$ is the reaction mechanism function. If $f(\alpha) = (1-\alpha)^n$, where n is the order of the reaction, then integration of eq 2 yields

$$\frac{AR}{\beta E_a}\left(1 - \frac{2RT}{E_a}\right)\exp\left(\frac{-E_a}{RT}\right) = \begin{cases} \ln\left(\dfrac{-\ln(1-\alpha)}{T^2}\right), n = 1 \\ \ln\left(\dfrac{1-(1-\alpha)^n}{(1-\alpha)T^2}\right), n > 1 \end{cases} \quad (3)$$

dx.doi.org/10.1021/ef2001772 |*Energy Fuels* 2011, 25, 1566–1570

Table 2. Calculated Activation Energies for Asphaltene Gasification/Cracking in the Presence and Absence of Metal Oxide Nanoparticles

temperature range		225−375 °C	375−455 °C	550−760 °C
virgin asphaltenes	E_a (kJ/mol)	49	130	41
	R^2	0.9871	0.9961	0.9921
asphaltenes adsorbed over nanoparticles		275−375 °C	375−440 °C	
NiO	E_a (kJ/mol)	46		
	R^2	0.9956		
Co_3O_4	E_a (kJ/mol)	56		
	R^2	0.9907		
Fe_3O_4	E_a (kJ/mol)	39	74	
	R^2	0.9906	0.9993	

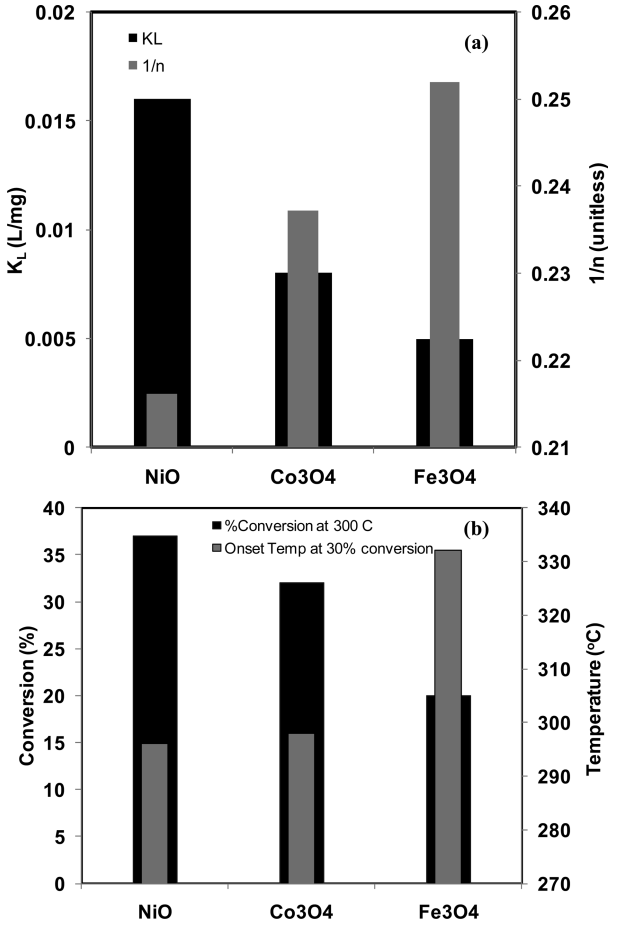

Figure 5. Relationship between adsorption affinity and catalytic activity of different nanoparticles: (a) Langmuir and Freundlich adsorption affinity constants (K_L and $1/n$, respectively) obtained from ref 5 and (b) percent conversion and gasification temperature of asphaltenes in the presence of nanoparticles.

where $\beta = dT/dt$. If n is known, then a plot of the right-hand side of eq 3 versus $1/T$ would give a straight line with a slope = E_a/R.[8] Nonetheless, some deviation from the straight line can occur because of the presence of competitive reactions or a change in the reaction mechanism with an increase in the temperature. However, this does not significantly impact the validity of the equation.[5,9−11] Figure 4 shows the plot of $\ln(-\ln(1-\alpha)/T^2)$ versus $1/T$. When this method is employed, the values of the activation energy were determined for oxidation of asphaltenes in the presence and absence of nanoparticles. The values determined are listed in Table 2. For virgin asphaltenes, the activation energy was calculated for three distinct temperature regions between 225 and 760 °C. As shown in Table 2, the activation energy and oxidation temperature of asphaltenes decreased significantly in the presence of nanoparticles. When adsorbed onto NiO and Co_3O_4 nanoparticles, asphaltenes oxidized completely before 350 °C. In the case of Fe_3O_4, the oxidation was less rapid, with activation energies listed in two temperature regions (Table 2).

3.3. Relationship between Adsorption Affinity and Catalytic Activity of Nanoparticles. Evidently, asphaltene adsorption and gasification/cracking are metal-oxide-specific. From the above-mentioned results, the presence of nanoparticles caused a drop in the activation energy and lowered the reaction temperature, hence, showing their catalytic effect. One interesting correlation was found to exist between the adsorption affinity constant and the catalytic activity. The results are described in Figure 5. Figure 5a shows the values obtained for adsorption affinity constants calculated for the three nanoparticles in our previous study using Langmuir and Freundlich adsorption models.[5] Regardless of the model used, the affinity constant was highest for NiO and lowest for Fe_3O_4. The affinity constant is a measure of the interaction between the adsorbate and adsorbent. The higher the value, the greater the strength of interaction. Figure 5b shows the measure of catalytic activity in terms of conversion at a given temperature and also in terms of the onset oxidation temperature at a given conversion (30%). NiO shows the highest conversion at a given temperature probably because the adsorbate−adsorbent interactions are the strongest. Fe_3O_4 shows the lowest catalytic activity and adsorption affinity. A comparison of panels a and b of Figure 5 shows that the catalytic activity is directly related to the affinity constant. The calculated percent conversion at the onset temperature for NiO, Co_3O_4, and Fe_3O_4 nanoparticles was 37, 32, and 21%, respectively. This indicates that asphaltene adsorption followed by catalytic steam gasification/cracking is strongly affected by the strength of the interaction between asphaltenes and various types of nanoparticles.

4. CONCLUSIONS

In this work, nanoparticles of Co_3O_4, Fe_3O_4, and NiO were employed for the adsorptive removal of asphaltenes from heavy oil model solution followed by asphaltene catalytic steam gasification/cracking. The nanoparticles tested showed high catalytic activity for asphaltene gasification/cracking. A correlation

appears to exist between the affinity constant and catalytic activity; the higher the affinity constant, the greater the catalytic activity. Among the tested nanoparticles, NiO nanoparticles showed the highest adsorption affinity and catalytic activity for asphaltenes.

AUTHOR INFORMATION

Corresponding Author
*E-mail: nassar@ucalgary.ca (N.N.N.); ppereira@ucalgary.ca (P.P.-A.).

ACKNOWLEDGMENT

Financial support provided by Carbon Management Canada, Inc. (CMC), a research network financed by the National Science and Engineering Research Council (NSERC), is gratefully acknowledged.

REFERENCES

(1) Government of Alberta, Canada. *Environmental Management of Alberta's Oil Sands*; http://environment.gov.ab.ca/info/library/8042.pdf (accessed on Aug 1, 2010).
(2) Pereira, P.; Romero, T.; Velasquez, J.; Tusa, A.; Rojas, I.; Camejo, W.; Rosa-Brussin, M. U.S. Patent 6,030,522, 2000.
(3) Pereira, P.; Marzin, R.; Zacarias, L.; Cordova, J.; Carrazza, J.; Marino, M. U.S. Patent 5,885,441, 1999.
(4) Carrazza, J.; Pereira, P.; Martinez, N. U.S. Patent 5,688,741, 1997.
(5) Nassar, N. N.; Hassan, A.; Pereira-Almao, P. *Energy Fuels* **2011**, *25*, 1017–1023.
(6) Nassar, N. N. *Energy Fuels* **2010**, *24*, 4116–4122.
(7) Hassan, A.; Carbognani, L.; Pereira-Almao, P. *Energy Fuels* **2010**, *24*, 5378–5386.
(8) Coats, A. W.; Redfern, J. P. *Nature* **1964**, *201*, 68–69.
(9) He, B. L.; Song, Q.; Xu, S.; Yao, Q. *Proceedings of the 5th Asia-Pacific Conference on Combustion*; The University of Adelaide: Adelaide, South Australia, Australia, 2005; pp 253−256.
(10) Li, J.; Yan, R.; Xiao, B.; Liang, D. T.; Du, L. *Environ. Sci. Technol.* **2008**, *42*, 6224–6229.
(11) Yanagisawa, K.; Suzuki, T. *Fuel* **1993**, *72*, 25–30.